



## **APPLYING 3D TECHNOLOGIES FOR EVALUATING WEAR OF SMALL-DIAMETER CORE DRILLING BITS**

### **APLIKÁCIA 3D TECHNOLOGIÍ NA VYHODNOTENIE OPOTREBOVANIA MALOPRIEMEROVÝCH KORUNIEK PRE JADROVÉ VRTANIE**

*Alexander Kiovský<sup>1</sup>, Edita Lazarová<sup>2\*</sup>, Mária Bali Hudáková<sup>3</sup>, Pavol Vavrek<sup>4</sup>, Vít'azoslav Krúpa<sup>5</sup>, Lucia Ivaničová<sup>6</sup>*

#### **Abstract**

The study focuses on the application of modern 3D technologies for evaluating the wear of a small-diameter diamond core bit following drilling on a laboratory drilling stand. Various surface scanning and 3D modeling approaches in *3DF Zephyr* are presented, along with their subsequent processing using specialized software. The results demonstrated that frontal scanning of the core bit with the *Discovery Artisan 1024* digital microscope provides a sufficiently detailed topographical representation of the surface for further analysis. Processing in *CloudCompare* enabled the creation of color-coded wear maps, determination of the distribution of changes on the cutting surface, and calculation of volumetric material loss. The proposed procedure represents an effective tool for comprehensive assessment of drill bit wear.

#### **Abstrakt**

Príspevok sa zaoberá využitím moderných 3D technológií pri hodnotení opotrebovania malopriemerovej diamantovej korunky po vrtaní na laboratórnom vrtnom stande. Predstavené sú rôzne možnosti snímania povrchu a tvorby 3D modelov v softvéri *3DF Zephyr*, ako aj ich následné spracovanie špecializovaným softvérom. Výsledky ukázali, že čelné snímanie korunky digitálnym mikroskopom *Discovery Artisan 1024* poskytuje dostatočne detailný plastický obraz povrchu pre ďalšie spracovanie. Analýzou v softvéri *CloudCompare* bolo možné vytvoriť farebné mapy opotrebovania, určiť rozloženie zmien na rozpojovacej ploche a vypočítať objemový úbytok materiálu. Navrhnutý postup predstavuje efektívny nástroj pre komplexné hodnotenie opotrebovania vrtnej korunky.

## **Keywords**

*Drilling, wear, small-diameter diamond core drill bits, 3D technologies*

## **Kľúčové slová**

*Vrtanie, opotrebovanie, malopriemerové jadrovacie diamantové korunky, 3D technológie*

## **1. Introduction**

Core rotary drilling represents an energy demand operation that is widely used primarily in mining geology, in the search and exploration of mineral deposits, in oil and natural gas exploration, as well as in foundation engineering and grouting boreholes. At present, diamond drill bits are predominantly used as the cutting tool, owing to their exceptional ability to disintegrate rock. (Tillmann, W., 2000; Tönshoff, H.K. et al., 2002).

The working surface of the research diamond drill bit consisted of a layer of embedded natural diamonds. The quantity and dimensions of these diamonds determine how the rock breaks into fragments and the shape of the resulting pieces. Drill bit matrices are made of high-quality, wear-resistant materials that retain the diamonds throughout the tool's service life. During operation, both the diamonds and the matrix are subjected to wear (Guttenkunst, E., 2018). The most frequent type of wear on the working surface is mechanical, predominantly abrasive and fatigue wear (Xuefeng, T. et al., 1994; Mostofi, M. et al., 2018). Investigation into the wear of diamonds in impregnated micro drill bits, and identification of factors contributing to this wear, has been conducted by Miller, D. et al. (1991).

Drill bit wear is influenced by the applied drilling regime (thrust, rotation speed) and depends on rock properties, the removal of drill cuttings, the proportion of fragmented rock fractions, the drilled length, and other factors (Plinninger et al., 2002). Wear affects the efficiency of rock fragmentation, increases the energy demand of drilling, reduces the drilling rate, shortens drill bit lifespan (Capik, M., 2021), and significantly elevates the economic costs of the drilling process (Wang, Z. et al., 2024).

Methods for assessing wear can be classified into two principal categories. The first group includes approaches designed to evaluate tool or material wear. Among these, 3D modeling and 3D scanning are particularly valuable, allowing detailed analysis of volumetric and mass changes (Abbas, K.R., 2018; Jones, M., 1995; He, L. et al. 2023). A simpler, though less accurate, method is weighing the tool before and after use, which provides basic quantification of mass loss (Miller et al., 1991; Malevich, 2021). The second group comprises methods for real-time process monitoring. Vibroacoustic techniques record vibrations and acoustic emissions during drilling, providing insights into tool dynamics (Karakus, M. et al., 2014; Ferrari, G. et al., 2015; Lazarová et al., 2020). More recently, artificial intelligence (AI) has been applied, utilizing signal processing and machine learning to predict tool condition and drilling progression (Perez, S. et al., 2017; Zhang, Q. et al., 2024). A comparison of these methods is presented in Table 1.

**Tab. 1 Comparison of methods used for monitoring and evaluating wear**

<b>Criterion</b>	<b>3D Modeling</b>	<b>Weighing</b>	<b>Vibroacoustic Methods</b>	<b>AI-Based Methods</b>
<b>Accuracy</b>	Very high (volume & geometry data)	Low–medium (overall mass)	Medium (indirect indicators)	Medium–high (depends on training)
<b>Cost &amp; Time Efficiency</b>	High cost, time-intensive (scanning, processing)	Very low cost, fast	Moderate cost (sensors), fast	High implementation cost; efficient long-term
<b>Automation Potential</b>	Limited (manual handling)	High (easily automated)	High (sensor integration)	Very high (software/autonomous)
<b>Real-Time Suitability</b>	Unsuitable (ex situ)	Unsuitable (ex situ)	Suitable (online signal analysis)	Suitable (real-time prediction)

The comparison shows that while 3D modeling provides the most accurate evaluation of wear, its high cost and time requirements limit routine or real-time application. Weighing is simple and cost-effective but less precise. Vibroacoustic and AI-based methods are more promising for online monitoring, with AI offering the highest potential for automation and predictive assessment.

Within the framework of experimental research on rock disintegration by drilling conducted at our research department, the need has emerged for rapid and precise evaluation of drill bit wear. One of the promising approaches is the use of 3D technologies—namely 3D scanning, photogrammetry, and software-based processing of 3D models generated from scanned tool surfaces. Our study is based on the hypothesis that modern 3D technologies enable more accurate quantification of wear compared to traditional methods. The application of these technologies allows us to:

- accelerate and refine the evaluation process,
- obtain new wear parameters,
- capture even very small surface changes of the tool (such as diamond polishing, abrasion, destruction, or gradual matrix wear),
- determine the degree of wear with greater accuracy,
- analyse archived 3D models to identify relationships between drilling parameters, rock properties, and the extent of wear.

The paper presents the devices employed for wear assessment using a non-contact measurement method, based on transferring scanned drill bit surfaces into a virtual 3D environment and subsequently processing them with specialized software.

## **2. Materials and methods**

The research was carried out under laboratory conditions. The primary objective was not to monitor the wear process in detail, but to select and validate an appropriate methodology for wear evaluation using 3D technologies. Drilling experiments were conducted on an experimental drilling rig.

## 2.1 Experimental drilling rig

The experimental device (Fig. 1) was designed and constructed at the Institute of Geotechnics of the Slovak Academy of Sciences to simulate the real drilling process without the influence of the drill string. The device is equipped with a specialized measurement system that controls operational parameters (rotation speed and thrust force), monitors, and archives the measured process variables (torque, rotation speed, thrust force, and drilling depth). The rotation speed of the drilling tool is adjustable by regulating the electric drive within the range of 0–2,220 rpm. The thrust force applied to the rock is continuously adjustable in the interval of 0–20,000 N and is measured by a dynamometer located at the contact point between the hydraulic cylinder and the sample holder. Drilling depth is measured using a magnetostrictive position sensor with an accuracy of  $\pm 0.2$  mm. For cuttings removal and as a flushing fluid, water was used in the experiments, with a flushing rate of  $10^{-3} \cdot \text{m}^3 \cdot \text{s}^{-1}$ . In automatic mode, the drilling rig is computer-controlled.



*Fig.1 Experimental laboratory horizontal drilling rig (left) and detail of sample holder and drilling tool (right)*

## 2.2 Drilling tool

For the purpose of wear assessment, a three-channel diamond core drill bit manufactured by URDIAMANT (Czech Republic) was selected. The drill bit had previously been used in other experimental trials. It was produced with diamond grains of 16–25 stones per carat, corresponding to a calculated diamond size of 1.89–1.63 mm. Three-channel surface-set diamond core drill bit, with an outer diameter of 46 mm and a core diameter of 32 mm was used for research purposes.

## 2.3 Rock specimens

For the investigation of rock disintegration by drilling and tool wear, two rock types were employed: limestone from the Včeláre quarry (Slovakia) and granodiorite from the Hradová quarry (Slovakia). The tested rock samples were shaped into rectangular blocks with dimensions of approximately  $150 \times 150 \times 260$  mm. The research was initially conducted using only limestone.

Limestone is a sedimentary and homogeneous rock. Based on the measured average uniaxial compressive strength of 85.1 MPa, it can be classified as a strong rock. Its measured abrasivity of  $0.0186 \text{ mg}\cdot\text{m}^{-1}$  ranks it among very weakly abrasive rocks. As no measurable wear was observed after drilling 27 limestone samples (5.4 m in total), the testing procedure was modified by alternating limestone with granodiorite specimens to accelerate drill bit wear. Granodiorite is an intrusive igneous rock with uniform grain size and a significant quartz content. According to ON 44 1121 (1982), the abrasivity measured in our laboratory was  $1.4092 \text{ mg}\cdot\text{m}^{-1}$ , which corresponds to a medium-abrasive rock. The average uniaxial compressive strength of 85.8 MPa also classifies it as a strong rock.

## 2.4 Drilling regime, scanning sequence, and 3D Model generation

The process parameters (applied thrust force and rotation speed) were not predefined according to a fixed experimental plan. Instead, the drilling regime was continuously adjusted throughout the experiments based on interim measurement results, as it was necessary to induce drill bit wear detectable by the instruments within a limited timeframe. The research was focused exclusively on monitoring drill bit wear using 3D technologies; therefore, the reproducibility of the experiments was not considered.

For both limestone samples (denoted as  $L$ ) and granodiorite samples ( $G$ ), an identical rotation speed of 1,000 rpm was applied. While the thrust force remained approximately constant during drilling of the limestone samples, it was gradually increased in the case of granodiorite samples in order to accelerate drill bit wear. To evaluate drill bit wear, four 3D surface scans of the drill bit were performed:

- $S_1$  – after drilling 27 limestone samples,
- $S_2$  – after completion of experiment  $G_1$ ,
- $S_3$  – after drilling four limestone samples ( $L_{28}$ – $L_{31}$ ) and one granodiorite sample ( $G_2$ ),
- $S_4$  – after completion of experiments  $L_{32}$  and  $G_3$ .

The acquired data were transferred into a virtual 3D environment, where they were processed by software and used to generate four 3D models  $M_1$ – $M_4$ .

**Tab. 2 Specification of drilling parameters, definition of scanning intervals, and procedure for 3D model generation**

Rock	$L_{27}$	Scanning $S_1$	$G_1$	Scanning $S_2$	$L_{28}$	$L_{29}$	$L_{30}$	$L_{31}$	$G_2$	Scanning $S_3$	$L_{32}$	$G_3$	Scanning $S_4$
Thrust force [N]	17,000		9,000		18,000	17,800	17,800	18,000	10,000		17,000	16,000	
Rotation speed [rpm]	1,000		1,000		1,000	1,000	1,000	1,000	1,000		1,000	1,000	
Experiment Drilled length [mm]	200		180		200	200	150	200	180		200	150	
Total drilled length [mm]	5,400	5,580	5,780	5,980	6,130	6,330	6,510	6,710	6,860				
3D model		$M_1$		$M_2$						$M_3$			$M_4$

Note: The tested drill bit had already been used prior to the present study for drilling 27 limestone samples ( $L_1$ – $L_{27}$ ) with a total drilled length of 5.4 m. For this reason, the indexing in Table 2 begins with experiment  $L_{27}$ .

Abbreviations used:  $L$  - Limestone,  $G$  - granodiorite,  $S$  - scanning,  $M$  - model (3D model).

Table 2 provides a chronological overview of the individual experiments, including the applied drilling parameters (rotation speed and thrust force), the drilled length of each sample, and the cumulative total drilled length. It also indicates the scanning of the drill bit surface and the subsequent generation of 3D models.

## 2.5 Devices used for 3D model generation in wear analysis

An application scheme of the tested devices used for drill bit wear evaluation is presented in Fig. 2.

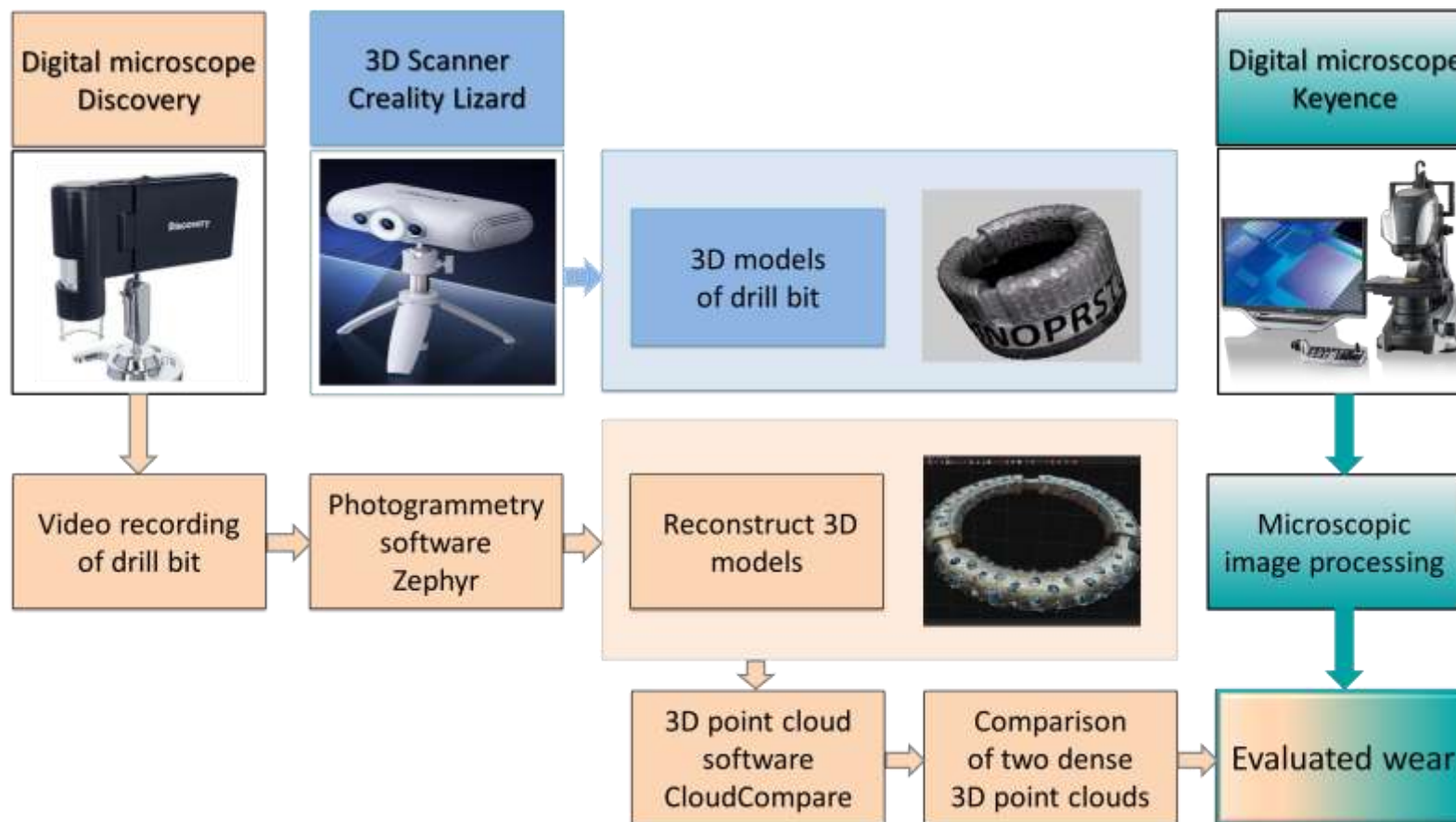


*Fig. 2 Application scheme of the tested devices used for drill bit wear evaluation*

For the purposes of this study, the following devices were tested:

- Creality CR-Scan Lizard 3D scanner,

- *Discovery Artisan 1024* digital microscope,
- *Keyence VHX-X1series* digital microscope.

### 3. Analysis of 3D modeling equipment for wear evaluation

For the purposes of this study, three devices designed for 3D surface digitization were tested. Their comparison primarily served to determine which of the tested devices was most suitable for investigating drill bit wear. The devices differ in technical complexity, accuracy, resolution, the level of detail captured, and cost. The following subsections present the three approaches: the use of the benchtop 3D scanner *Creality CR-Scan Lizard*, the digital microscope *Discovery Artisan 1024*, and the specialized 3D microscope *Keyence VHX-X1*.

#### 3.1 *Creality CR-Scan Lizard* – benchtop 3D scanner

The *Creality CR-Scan Lizard* is designed for precise object scanning with a resolution of 0.1 mm and accuracy of 0.05 mm, suitable for digitalizing objects the size of drill bits. It provides several scanning modes, a working distance of 150–400 mm, and a frame rate of 10 fps. The integrated light source combines LED and NIR, and output formats include OBJ, STL, and PLY. The scanner is accompanied by *CRStudio* software for scanning, 3D model generation, and editing.

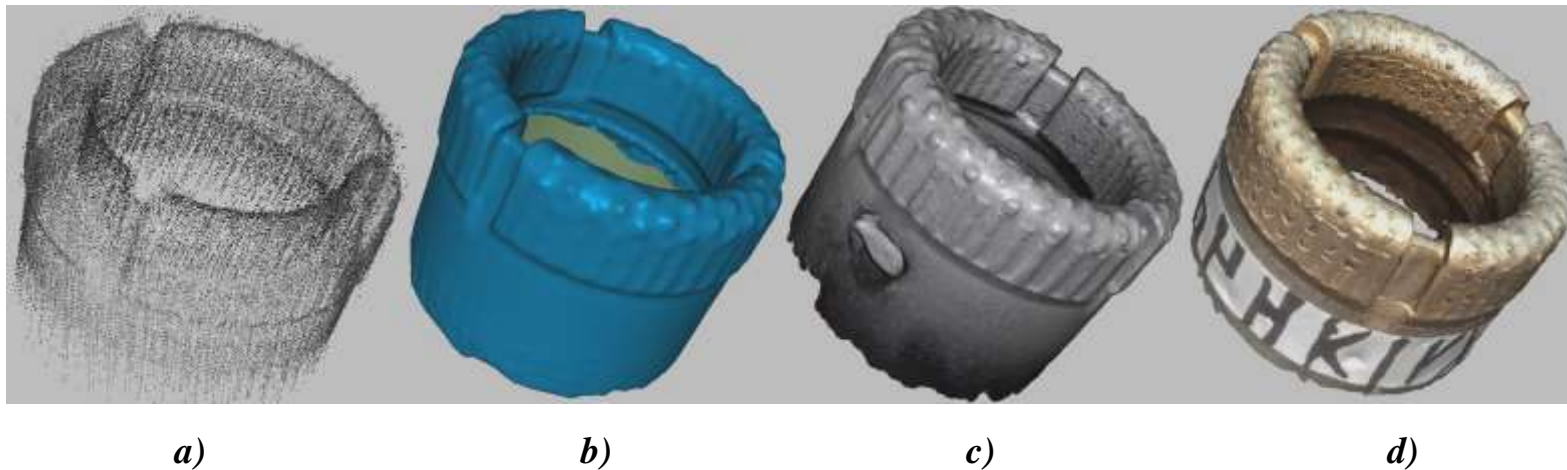


**Fig. 3** *Process of creating a 3D model: a) point cloud, b) 3D representation, c) monochromatic texture, d) color texture with reference markers*

During scanning, the *Creality CR-Scan Lizard* was fixed on a stand, while the drill bit was placed on a rotating table. A contrast layer was applied to its surface using a dedicated scanning spray. To obtain high-quality records, it was necessary to optimize several parameters, including light intensity, background color, scanning angle, distance between the scanner and the bit, scanning depth, and rotation speed of

the turntable. The best results were achieved at a rotation speed of 2 rpm. The scanning output is a point cloud (Fig. 3a). In the next step, the neighboring points of the cloud are connected into meshes, resulting in a 3D representation (Fig. 3b). The scanner itself does not allow for color scanning; however, its software makes it possible to capture the texture simultaneously with an external color camera and add it to the 3D model. Adding the internal texture provided a more accurate monochromatic representation of the drill bit (Fig. 3c), whereas adding the external texture produced a color representation (Fig. 3d). In Fig. 3d, auxiliary markers placed on the scanned bit are also visible, which are essential for creating the 3D model from the scanned data and for synchronizing multiple 3D models.

It was found that despite the declared scanning accuracy of 0.05 mm, the generated 3D models were not sufficiently detailed for a reliable evaluation of drill bit wear.

### 3.2 *Discovery Artisan 1024* – digital microscope

The *Discovery Artisan 1024* is a portable device with a 5 MP camera, offering 10–300× optical magnification and up to 1,200× digital zoom. It supports still images and Full HD video, with eight adjustable LEDs around the lens for optimal lighting. In this study, the video function was used at a fixed distance of 9.8 cm and 10× optical magnification.

For the creation of 3D models, two approaches to scanning the drill bit surface were applied. The choice of method was based on the obtained results. Initially, detailed scanning in sections was performed, later followed by frontal surface scanning, which proved to be more suitable.

#### a) *Scanning the drill bit in sections*

The surface of the bit was scanned with the *Discovery Artisan 1024* digital microscope at 10× magnification, which improved the resolution of the captured details.

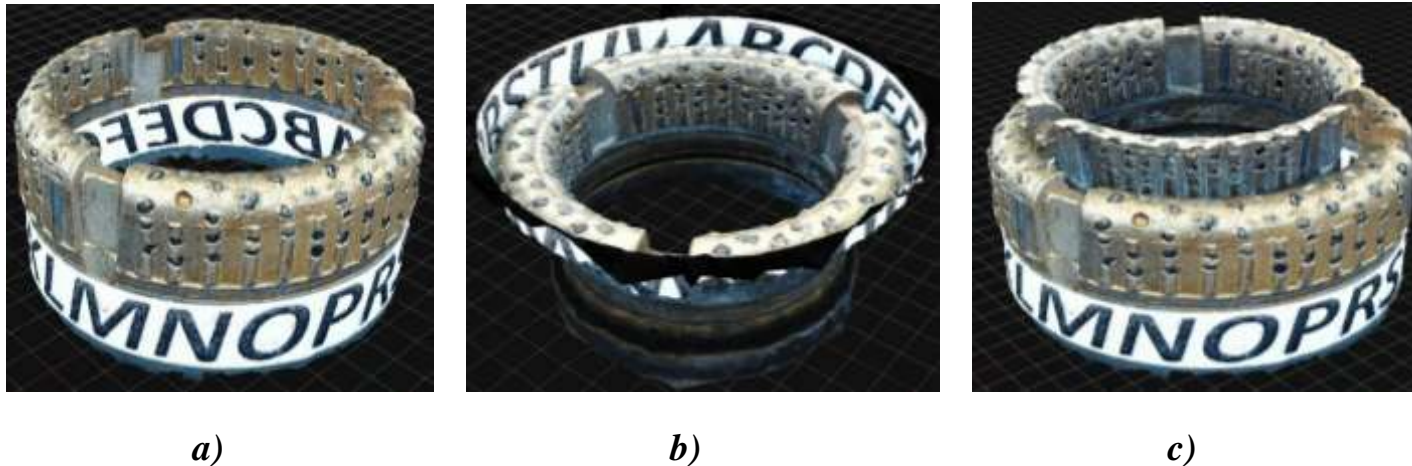


**Fig. 4** Stages of 3D surface reconstruction by merging: a) outer surface, b) inner surface, c) combined object

To ensure consistent recording, identical lighting conditions, the same rotation speed of the rotary table (2 rpm), and constant positioning and distance from the lens were maintained. The recording was made in the form of a video and subsequently processed in the 3DF *Zephyr* software. However, the shallow depth of field of the microscope lens did not allow capturing the entire cutting surface of the bit at once. Therefore, the inner surface (Fig. 4a) and the outer surface (Fig. 4b) of the bit were scanned separately. The *Zephyr* software, however, was unable to accurately merge these two 3D models into a single unit, which is necessary for their comparison. Fig. 4 shows the result of separate scanning of both surfaces and their merging.

*b) Frontal scanning of the drill bit surface*

Based on the experience from the first approach, it was found that for spatial visualization of the worn drill bit surface it is sufficient to capture only its frontal surface. The optical parameters of the microscope and the scanning method provide a plastic output of the scanned surface of sufficient quality for our purposes (Fig. 5), which can be further improved by using a tilting stand.

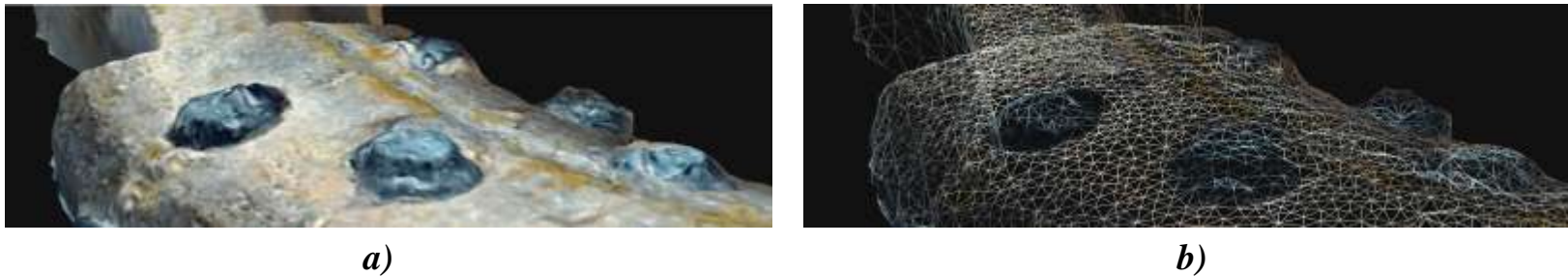


**Fig. 5 Magnified 3D surface model obtained by frontal scanning: a) surface with texture, b) surface with 3D mesh**

The captured frontal surface was further processed using the *Zephyr* software. Individual frames were extracted from the video recording at a frequency of 2 frames per second. The resulting 3D model was created by comparison, i.e., by identifying common points between the frames and transforming them from two-dimensional image data into three-dimensional space. The final phase of the 3D modeling process was the virtual reconstruction of the object surface. The 3D models exported from *Zephyr* correspond to the actual size of the scanned object (drill bits) in millimeters.

The creation of a 3D model from sequential video frames is illustrated in Fig. 6, where the blue markers indicate the position of the individual frame sources around the object, which serve to reconstruct its three-dimensional model.

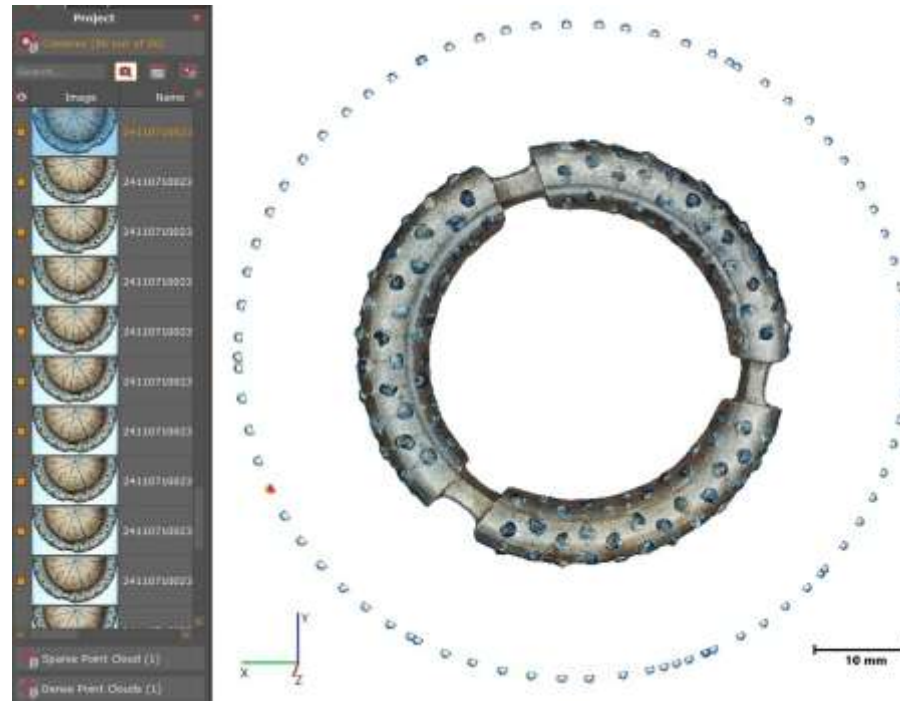


*Fig. 6 Creation of 3D model  $M_1$ : left – extracted sequential frames, right – positions of image sources, center – reconstructed 3D model*

### 3.3 Keyence VHX-X1 – specialized 3D microscope

The specialized digital 3D microscope *Keyence VHX-X1* was also tested for creating 3D models and evaluating the wear of small-diameter drill bits. It offers a total depth of field of up to 46 mm, features automatic focusing, and, thanks to its tilting objective lens, enables imaging of the drill bit surface from multiple angles. The software provides automatic depth annotation and depth-based color scaling, allowing the generation of surface profiles with volume calculations for marked areas, as well as overall evaluation of differences between two models.

Fig. 7 illustrates the process of generating a profile on a selected section of the drill bit's cutting segment. The yellow line in the left image indicates the location of the desired profile. The middle image shows a 3D representation of the marked section with corresponding depths. The right image displays the roughness height curve along the marked profile, with the y-axis representing roughness heights in millimetres and the x-axis representing distances from the internal edge of the drill bit.

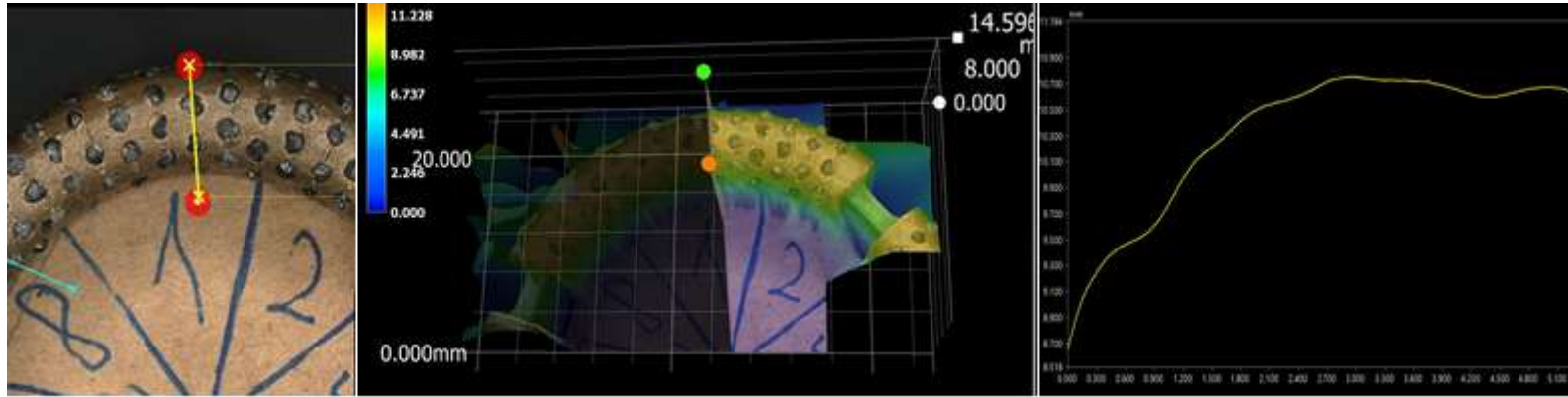


**Fig. 7** *Transverse profile of the marked section of the drill bit's cutting segment in the coordinate system*

For the purposes of this study, the *Keyence VHX-X1* proved to be the most suitable device for precise wear assessment; however, due to its high acquisition cost, routine use for this application would be economically impractical.

#### **4. Use of the selected device and results evaluation**

The analysis of 3D models obtained from the *Crealty CR-Scan Lizard* 3D scanner showed that they are not suitable for further processing in *CloudCompare*, mainly due to their insufficient ability to capture details.

The digital microscope *KEYENCE VHX-X1* provides high-quality outputs, and its software enables fast evaluation; however, its acquisition costs are too high for this purpose.

Therefore, we chose an approach in which 3D models were created by frontal scanning with the *Discovery Artisan 1024* digital microscope. The acquired sequential images were subsequently processed in *3DF Zephyr* software, which generated the 3D model (Fig. 6). The created models were then analyzed in *CloudCompare*.

To compare the surfaces of the drill bit, the *Cloud-to-Mesh (C2M)* method was used. First, both models were aligned, and the surface change was calculated by measuring the distance between the point cloud of the first 3D model and the reference 3D mesh of the second model. Fig. 8 shows two compared 3D models –  $M_1$  after drilling 27 limestone samples  $L_1-L_{27}$  a  $M_2$  after drilling sample  $G_1$  (Table 2).

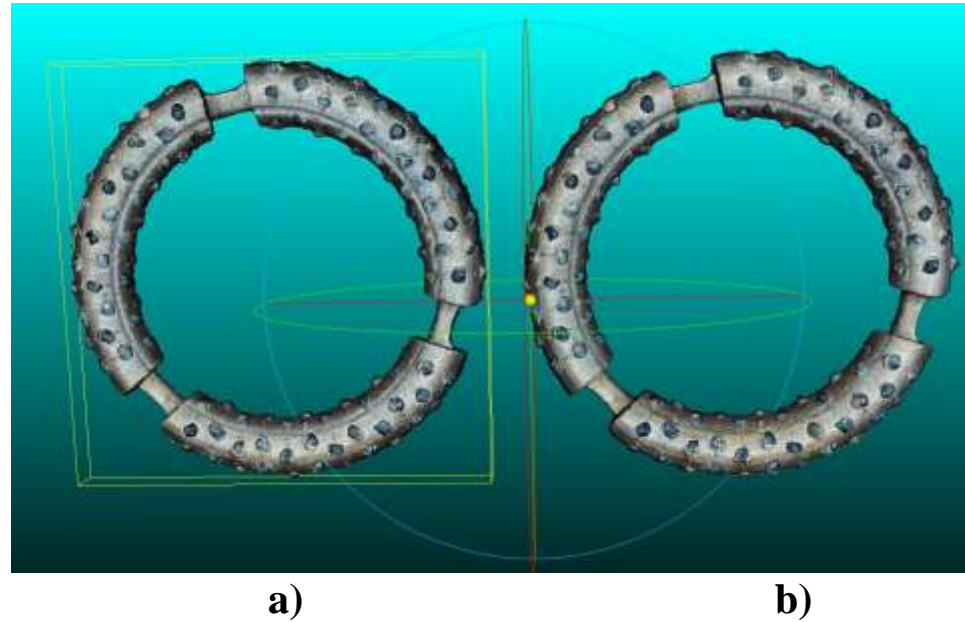


**Fig. 8 3D models analyzed in CloudCompare software; a) model  $M_1$ , b) model  $M_2$**

The result of the comparison between models  $M_1$ – $M_2$  is shown in Fig. 9. The histogram on the left side of the figure illustrates the distribution of height differences between the two drill bit surfaces. The X-axis represents the deviations between the compared surfaces (in millimeters). The calculated mean deviation is +0.024 mm with a standard deviation of 0.051 mm, which means that most points deviate only by a few hundredths of a millimeter. The Gaussian curve (black line) indicates that the distribution of deviations has an approximately normal character, with most points concentrated around the mean. Minor asymmetries or deviations from the ideal Gaussian curve suggest the presence of local areas with greater wear.

The surface color map (right side of Fig. 9) shows the drill bit viewed from above with a color-coded distribution of deviations. Most of the surface is green, representing minimal wear. Red areas indicate the greatest material loss, while blue areas represent negative deviations. The negative values result from the calculation method ( $C2M$ ), which assigns signs based on the orientation of surface normals, as well as from measurement noise or small shifts during surface alignment. The surface exhibits heterogeneity – wear is not evenly distributed but locally concentrated.

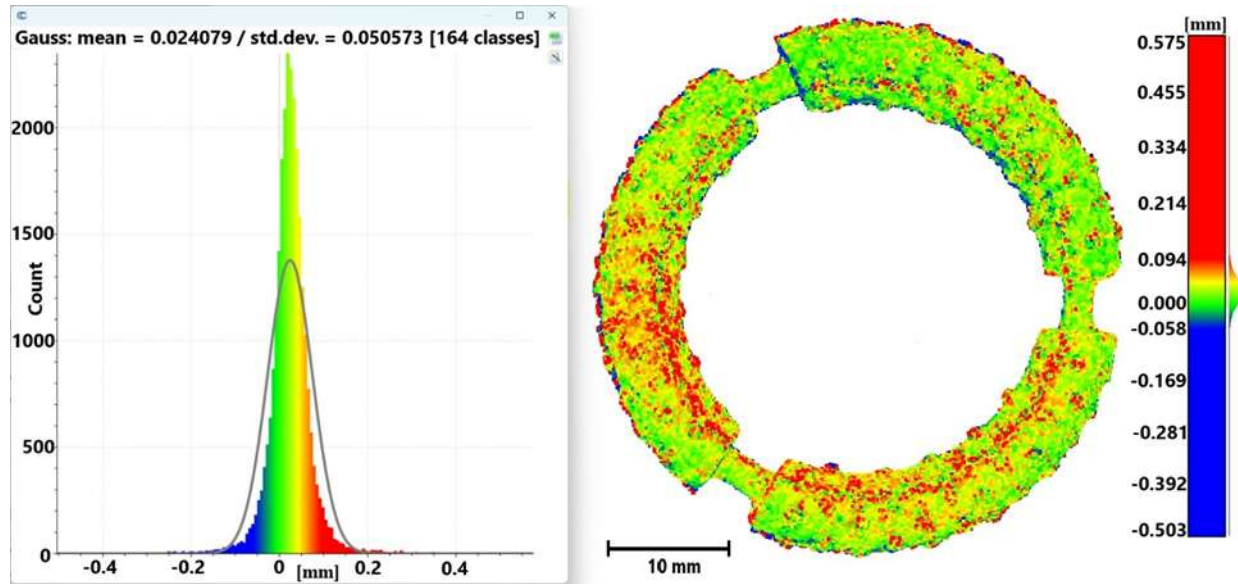


**Fig. 9 Wear analysis– comparison of models  $M_1$ – $M_2$ : histogram of deviations (left) and deviation color map (right)**

Subsequently, additional model pairs were analyzed. Fig. 10 presents the results of the comparisons  $M_1$ – $M_2$ ,  $M_2$ – $M_3$ , and  $M_3$ – $M_4$ , illustrating the progressive development and intensity of wear of the examined drill bit.

The individual models were generated according to the drilled lengths given in Table 2 as follows:

- $M_1$ : after drilling 5,400 mm of limestone,
- $M_2$ : after drilling 5,400 mm of limestone and 180 mm of granodiorite (total 5,580 mm),
- $M_3$ : after drilling 6,150 mm of limestone and 360 mm of granodiorite (total 6,510 mm),
- $M_4$ : after drilling 6,350 mm of limestone and 510 mm of granodiorite (total 6,860 mm).

The color scale is not uniform across all three images. It is dynamically adjusted according to the evaluated wear range. Each image exhibited a different maximum detected wear; therefore, the scale was adapted to utilize the full color spectrum and to enhance the visualization of details. Red always indicates the maximum within a given comparison, while blue represents the minimum.

The difference map generated from the first evaluation (model  $M_1$ – $M_2$ ), Fig. 10a, is predominantly green-yellow. The maximum wear depth reached only approximately 0.102 mm. The color contrast indicates the presence of local differences on the surface, although the overall material loss is minimal.

From the second evaluation (model  $M_2$ – $M_3$ ), Fig. 10b, it is evident that the maximum wear depth increased to approximately 0.130 mm. The entire spectrum shifted upward, indicating more pronounced wear, yet still not uniformly distributed. Differences between

segments remain observable. The non-uniformity of wear is more apparent—one segment exhibits the highest loss, whereas other parts of the drill bit remain within the range of minimal wear. This contrast reflects the unequal loading of segments during drilling.

The third evaluation (model  $M_3-M_4$ ), Fig. 10c, shows a maximum wear depth of approximately 0.179 mm, nearly double that observed in the first evaluation. Wear is now approaching a uniform distribution, as evidenced by larger red-yellow areas, indicating that wear is not only more severe but also more widespread, with material loss becoming more evenly distributed across the entire circumference. Blue areas (zones of minimal wear) are now observed only sporadically.

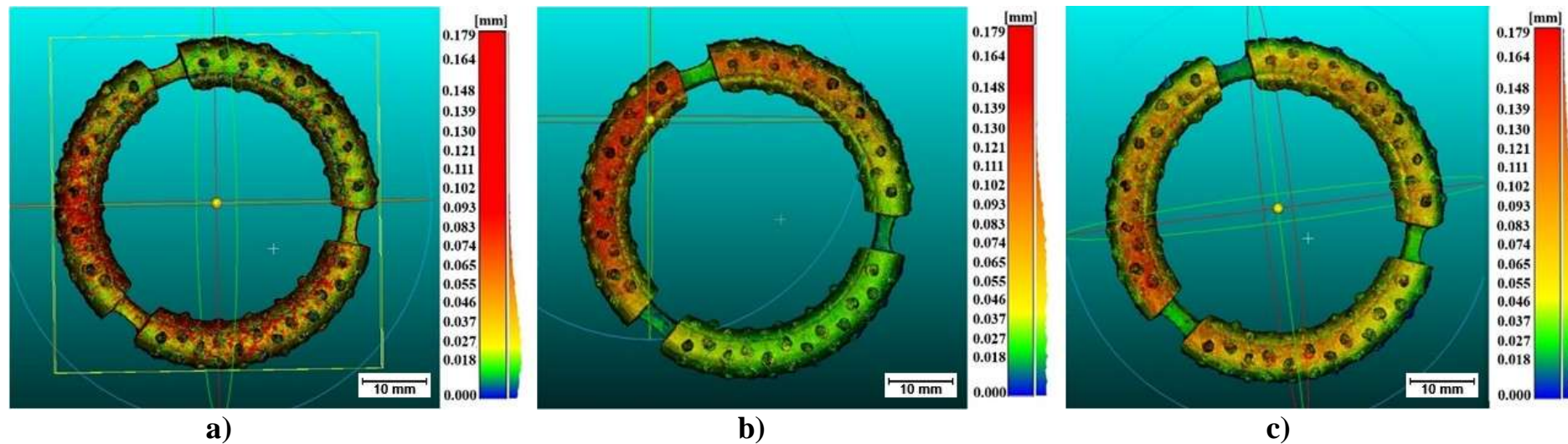


**Fig. 10 Results of wear monitoring – comparison of models a)  $M_1-M_2$ ; b)  $M_2-M_3$ ; c)  $M_3-M_4$**

These results demonstrate that with increasing drilling length, both the extent and nature of wear intensified. The observed incremental increase (0.102 – 0.130 – 0.179 mm) indicates a progressive growth of maximum material loss across successive evaluations. The relative distribution of colors further reveals an evolution in wear characteristics: from local and non-uniform, through extended but non-uniform, to an almost uniform wear pattern. Although the scales are not standardized, this progressive increase provides clear evidence that wear expanded and became more evenly distributed.

To quantify volumetric changes (Štroner, M. et al., 2019) the *Compute 2.5D Volume* function in *CloudCompare* was employed, producing the results presented in Fig. 11. In the left part of the figure, the calculation settings are shown, including the definition of the reference surface and the compared surface, the grid size, and the method for averaging values. For optimal accuracy, these parameters must be carefully adjusted—selecting the smallest possible grid density while maximizing the coverage of the analyzed volume shape in percentage terms.

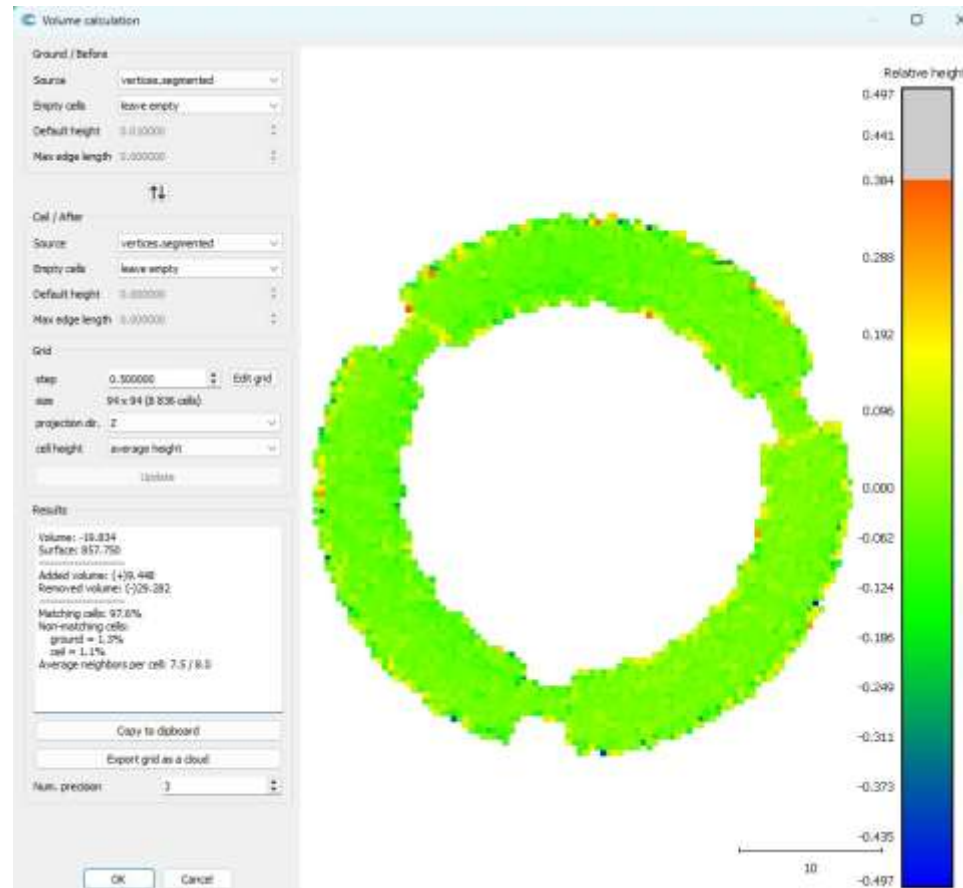


**Fig. 11** CloudCompare 2.5D volume analysis; Model  $M_1$ - $M_2$ : settings, deviation map, color scale, and quantitative results

The central part of Fig. 11 displays a color map of deviations from a top view of the drill bit, with the color scale on the right indicating the relative magnitude of deviations. The lower part of the window provides the quantitative results: the material loss volume (29.282 mm<sup>3</sup>), the volume gain (9.448 mm<sup>3</sup>), and their difference, representing the net calculated material loss, which amounts to 19.834 mm<sup>3</sup>.

The material volume losses calculated by the software are presented in Table 3. The table also includes the corresponding drill bit mass losses, which were determined by weighing under identical conditions using high-precision scales. Prior to weighing, the drill bits

were cleaned and dried for two hours in a laboratory oven at 110 °C. No alternative methods for assessing wear were employed in this study.

**Table 3 Material volume and mass losses of drill bits**

<b>Evaluation</b>	<b>Mass [g]</b>	<b>Volume [mm<sup>3</sup>]</b>	<b>Interval length [mm]</b>	<b>Total drilled length in study [mm]</b>	<b>Cumulative drilled length by bit [mm]</b>
$M_1 - M_2$	0.03	19.8	180	180	5,580
$M_2 - M_3$	0.04	31.7	930	1,110	6,510
$M_3 - M_4$	0.05	7.11	350	1,460	6,860

*Note: Interval Length represents the distance drilled between successive scans and the generation of 3D models; Total Drilled Length in study indicates the total distance drilled during this experiment; Cumulative Length to the total distance already drilled by the bit*

The wear measurements obtained from the comparisons of successive 3D models are summarized in Table 3, which shows that both mass loss and material volume removal increased with drilling, highlighting the progressive nature of wear.

When comparing models  $M_1$  and  $M_2$ , a mass loss of 0.03 g and a removed material volume of 19.6 mm<sup>3</sup> were observed after drilling 180 mm from the first scan ( $S_1$ ). The results from models  $M_2$  to  $M_3$ , after drilling 930 mm of rock between evaluations, showed a further increase in wear, with a mass loss of 0.04 g and a volume loss of 31.7 mm<sup>3</sup>, representing the most significant wear among the monitored intervals. From the start, a total of 1,100 mm of rock had been drilled. The final interval, between  $M_3$  and  $M_4$ , exhibited a mass loss of 0.05 g, but a smaller volume of removed material 7.11 mm<sup>3</sup> over a drilled length of 350 mm between evaluations.

The highest material loss was recorded between the  $M_2$  and  $M_3$  evaluations. In contrast, the final interval between  $M_3$  and  $M_4$  showed a continued decrease in mass, yet this was accompanied by only a minor reduction in volume. Wear is now evident around the entire circumference of the drill bit, as the matrix has also begun to wear. This finding is clearly illustrated in Fig. 10c.

These results demonstrate the capacity of 3D modeling to capture both quantitative and spatial aspects of drill bit wear, providing more detailed insights than conventional weighing alone.

## 5. The analysis and discussion

The primary aim of the experiment was not to monitor the wear process in detail, but to select and validate a suitable methodology for its assessment using 3D technologies. Previously, our laboratory primarily relied on conventional weighing, which, although simple and time-efficient, only provides a global measure of material loss and does not capture local changes in the cutting segments of the drill bit. This represents a significant limitation when studying wear mechanisms, as detailed geometry and microscopic surface changes are crucial for assessing tool lifetime.

To evaluate the suitability of the methodology, it was necessary to achieve measurable wear within a reasonable timeframe and extent. Therefore, the experimental conditions were modified: less abrasive limestone was replaced with granodiorite, and the applied force was increased from 9,000 N to 16,000 N. This allowed for faster degradation of the cutting segments and improved conditions for testing the accuracy and sensitivity of 3D scanning.

The results indicate that drill bit wear did not progress linearly, but with varying intensity across different drilling intervals. The largest volumetric loss was observed in the  $M_2$ – $M_3$  interval. The detected asymmetry and progressive nature of wear have a direct impact on drill bit lifetime. Asymmetric wear was caused by the mechanism of mounting the bit onto the thread. The threads of the clamping device and the seating surface of the drill bit show slight wear, and repeated drilling appears to induce small but increasing misalignment. Improper clamping can lead to premature wear of the cutting surface, reducing overall tool usability. Data analysis revealed that optimizing the clamping method and monitoring wear in the early phases are crucial, as degradation accelerates with increasing drilled length. The use of *C2M* allows the identification of localized areas with more intense wear, while the total material loss can be quantified with the module *Compute 2.5D Volume*. This combination provides both spatial and quantitative insights into wear patterns, offering a more comprehensive evaluation than conventional methods.

The present study did not systematically investigate the influence of drilling parameters or geological conditions on wear, but focused on the methodological selection of the most suitable 3D tool for future research. Comparisons confirmed that 3D digital modeling is an effective tool for quantitatively assessing drill bit wear. Compared to traditional weighing, it not only enables the determination of mass loss but also allows detailed mapping of its spatial distribution. This approach provides higher informational value by capturing asymmetric and localized surface changes, which significantly affect drilling efficiency. Furthermore, 3D scanning enables the creation of a virtual drill bit model and repeated measurements to compare its condition at different wear stages, including quantitative analyses (e.g., volume loss or area of worn zones).

The methodology can also be adapted for impregnated and smaller carbide bits, opening the way for broader application in geological and mining practice. The introduction of 3D digital technologies represents a significant step toward optimizing drill bit lifetime and more efficient drilling process management. Limitations of the method mainly involve the technical complexity of handling the entire process. Another limitation is that it is currently applicable only for post-drilling analysis, rather than real-time monitoring.

## 6. Conclusion

The experimental results confirmed that 3D digital methods provide significantly more accurate and comprehensive data on drill bit wear than traditional weighing or simple linear measurements. The use of the *Discovery Artisan 1024* digital microscope in combination with *3DF Zephyr* and *CloudCompare* software enabled not only the quantification of material volume loss but also precise visualization of its distribution on the cutting surface. Color difference maps between individual 3D models revealed the gradual increase of wear and the change in its character from localized to widespread.

It was demonstrated that this method is suitable for detailed analysis of drill bit geometric changes, documentation of microscopic defects, and monitoring wear dynamics. The obtained data provide a reliable basis for further research focused on the relationship between wear and rock type, drilling parameters, and the degradation rate of diamond bits.

In practice, the method proves useful for ongoing tool wear monitoring, optimization of drilling parameters based on segment wear analysis, prediction of bit lifespan, and more efficient planning of tool replacement. The documentation of results can also serve as a foundation for design modifications of diamond bits.

## Acknowledgements

This research was supported by projects VEGA 2/0090/23 and APVV-23-0364.

## References:

- ABBAS, R., K. (2018). A review on the wear of oil drill bits (conventional and the state of the art approaches for wear reduction and quantification). *Engineering Failure Analysis*, 90, 554–584. <https://doi.org/10.1016/j.engfailanal.2018.03.026>
- CAPIK, M., YILMAZ, A. O. (2021). Development models for the drill bit lifetime prediction and bit wear types. *International Journal of Rock Mechanics and Mining Sciences*, 139, 104633. <https://doi.org/10.1016/j.ijrmms.2021.104633>
- FERRARI, G., GÓMEZ, M. P. (2015). Correlation Between Acoustic Emission, Thrust and Tool Wear in Drilling. *Procedia Materials Science*, 8, 693–701. <https://doi.org/10.1016/j.mspro.2015.04.126>
- GUTTENKUNST, E. (2018). *Study of the wear mechanisms for drill bits used in core drilling*. <https://api.semanticscholar.org/CorpusID:52234137>
- HE, L., YAN, Z., HU, Q., XIANG, B., XU, H., BAI, Y. (2023). Rapid assessment of slope deformation in 3D point cloud considering feature-based simplification and deformed area extraction. *Measurement Science and Technology*, 34(5), 55201.
- JONES, M. W. (1995). 3D Distance from a Point to a Triangle. Department of Computer Science, University of Wales Swansea Technical Report CSR-5, 5. <https://doi.org/10.5281/zenodo.14173322>
- KARAKUS, M., PEREZ, S. (2014). Acoustic emission analysis for rock–bit interactions in impregnated diamond core drilling. *International Journal of Rock Mechanics and Mining Sciences*, 68, 36–43. <https://doi.org/10.1016/j.ijrmms.2014.02.009>
- LAZAROVÁ, E., KRULÁKOVÁ, M., LABAŠ, M., IVANIČOVÁ, L., FERIANČIKOVÁ, K. (2020). Vibration signal for identification of concrete drilling process and drill bit wear. *Engineering Failure Analysis*, 108. <https://doi.org/10.1016/j.engfailanal.2019.104302>
- MALEVICH, N., MÜLLER, C. H., DREIER, J., KANSTEINER, M., BIERMANN, D., DE PINHO FERREIRA, M., TILLMANN, W. (2021). Experimental and statistical analysis of the wear of diamond impregnated tools. *Wear*, 468–469, 203574. <https://doi.org/10.1016/j.wear.2020.203574>

- MILLER, D., BALL, A. (1991). The wear of diamonds in impregnated diamond bit drilling. *Wear*, 141(2), 311–320.  
[https://doi.org/https://doi.org/10.1016/0043-1648\(91\)90276-Z](https://doi.org/https://doi.org/10.1016/0043-1648(91)90276-Z)
- MOSTOFI, M., RICHARD, T., FRANCA, L., & YALAMANCHI, S. (2018). Wear response of impregnated diamond bits. *Wear*, 410–411, 34–42. <https://doi.org/10.1016/j.wear.2018.04.010>
- PEREZ, S., KARAKUS, M., PELLET, F. (2017). Development of a Tool Condition Monitoring System for Impregnated Diamond Bits in Rock Drilling Applications. *Rock Mechanics And Rock Engineering*, 50(5), 1289–1301. <https://doi.org/10.1007/s00603-016-1150-6>
- PLINNINGER, R. J., SPAUN, G. O., THURO, K. (2002). *Prediction And Classification Of Tool Wear In Drill And Blast Tunnelling*.  
<https://api.semanticscholar.org/CorpusID:54508902>
- ŠTRONER, M., KŘEMEN, T., BRAUN, J., URBAN, R., BLISTAN, P., KOVANIČ, Ľ. (2019). Comparison of 2.5d volume calculation methods and software solutions using point clouds scanned before and after mining. *Acta Montanistica Slovaca*, 24, 296–306.
- TILLMANN, W. (2000). Trends and market perspectives for diamond tools in the construction industry. *International Journal of Refractory Metals and Hard Materials*, 18(6), 301–306. [https://doi.org/https://doi.org/10.1016/S0263-4368\(00\)00034-2](https://doi.org/https://doi.org/10.1016/S0263-4368(00)00034-2)
- TÖNSHOFF, H. K., HILLMANN-APMANN, H., ASCHE, J. (2002). Diamond tools in stone and civil engineering industry: Cutting principles, wear and applications. *Diamond and Related Materials*, 11(3–6), 736–741. [https://doi.org/10.1016/S0925-9635\(01\)00561-1](https://doi.org/10.1016/S0925-9635(01)00561-1)
- WANG, Z., SUN, W., KANG, J., TAO, Y., TAN, S., DUAN, L. (2024). Influence of drilling technology on wear evolution of impregnated diamond bits. *International Journal of Refractory Metals and Hard Materials*, 123, 106793.  
<https://doi.org/10.1016/j.ijrmhm.2024.106793>
- XUEFENG, T., SHIFENG, T. (1994). The wear mechanisms of impregnated diamond bits. *Wear*, 177(1), 81–91.  
[https://doi.org/https://doi.org/10.1016/0043-1648\(94\)90120-1](https://doi.org/https://doi.org/10.1016/0043-1648(94)90120-1)
- ZHANG, Q., ZHENG, Z., HUANG, Z., SONG, X., WU, L., ZHANG, Z. (2024). Real-Time Recognition Of Drill Bit Wear State Using Clustering Algorithm And Gru Neural Network. *Proceedings of ASME 2024 43RD International Conference on Ocean, Offshore and Artic Engineering, OMAE2024, VOL 8*.

---

**Authors:**

<sup>1</sup>Ing. Alexander Kiovský – Institute of Geotechnics SAS, Watsonova 45, 040 01 Kosice, Slovakia, [kiovsky@saske.sk](mailto:kiovsky@saske.sk)

<sup>2\*</sup>Ing. Edita Lazarová, PhD. – Institute of Geotechnics SAS, Watsonova 45, 040 01 Kosice, Slovakia, [lazarova@saske.sk](mailto:lazarova@saske.sk) (corresponding author)

<sup>3</sup>Ing. Mária Bali Hudáková, PhD. – Institute of Geotechnics SAS, Watsonova 45, 040 01 Kosice, Slovakia, [krulakova@saske.sk](mailto:krulakova@saske.sk)

<sup>4</sup>Ing. Pavol Vavrek, PhD. – Institute of Geotechnics SAS, Watsonova 45, 040 01 Kosice, Slovakia, [vavrek@saske.sk](mailto:vavrek@saske.sk)

<sup>5</sup>Ing. Vít'azoslav Krúpa, DrSc. – Institute of Geotechnics SAS, Watsonova 45, 040 01 Kosice, Slovakia, [krupa@saske.sk](mailto:krupa@saske.sk)

<sup>6</sup>Ing. Lucia Ivaničová, PhD. – Institute of Geotechnics SAS, Watsonova 45, 040 01 Kosice, Slovakia, [ivanic@saske.sk](mailto:ivanic@saske.sk)